Depth-resolved soft x-ray photoelectron emission microscopy in nanostructures via standing-wave excited photoemission

F. Kronast[1], R. Ovsyannikov[1], A. Kaiser[2], C. Wiemann[2], S.-H. Yang[3],

A. Locatelli[4], D. E. Bürgler[3], R. Schreiber[3], F. Salmassi[5], P. Fischer[5],

H.A. Dűrr[1], C. M. Schneider[2],W. Eberhardt[1] and C. S. Fadley[2,5,6]

[1]BESSY mbH, Albert-Einstein-Str. 15, 12489 Berlin, Germany

[2]Forschungzentrum Jülich GmbH, IFF-9, 52425 Jülich, Germany

[3]Almaden Research Center, San Jose, CA 95120 USA

[4]Elettra, Sincrotrone Trieste S.C.p.A., 34012 Basovizza, Trieste, Italy

[5]Lawrence Berkeley National Laboratory, Berkeley, CA 94720, USA

[6]University of California, Davis, CA 95616, USA

Corresponding author: Florian Kronast

Address: BESSY mbH, Albert-Einstein-Str. 15, 12489 Berlin, Germany

e-mail : kronast@bessy.de

Phone: (+49) 30 6392 4620

Fax: (+49) 30 63924980

Abstract

We present an extension of conventional laterally resolved soft x-ray photoelectron emission microscopy. A depth resolution along the surface normal down to a few Å can be achieved by setting up standing x-ray wave fields in a multilayer substrate. The sample is an Ag/Co/Au trilayer, whose first layer has a wedge profile, grown on a Si/MoSi2 multilayer mirror. Tuning the incident x-ray to the mirror Bragg angle we set up standing x-ray wave fields. We

demonstrate the resulting depth resolution by imaging the standing wave fields as they move through the trilayer wedge structure.

The soft x-ray photoelectron emission microscope (PEEM), has emerged as a very powerful synchrotron-radiation based characterization tool in the past decade[1]. By imaging via core-level excitation of photoelectrons or secondary electrons, the technique is element specific, so that each constituent in a complex sample can be imaged separately. If the polarization of the radiation is altered, the magnetic state of each element can also be imaged via magnetic dichroism [2-4]. Time-resolved studies of magnetic switching are also possible[5, 6]. The lateral (x, y) resolution in such microscopes has reached 20nm, with instruments promising resolutions down to 1- 3nm [7]. However, a limitation in current PEEM measurements lies in the vertical resolution. Some vertical resolution is possible if a given element is known a priori to be at a certain depth below the surface, or if it exhibits some spectroscopic chemical signature as a function of depth, but in general the resolution in this dimension is not quantitative.

We have experimentally demonstrated the ability to add vertical resolution to PEEM imaging by using a soft x-ray standing wave (SW) as the exciting radiation. We combine a synthetic multilayer soft x-ray mirror of nm-scale periodicity as the sample substrate with a sample whose first layer has a wedge profile, as shown in Fig. 1[8, 9]. With this standing wave/wedge ("swedge") method, it has been possible in prior experiments to determine depth profiles of concentration, magnetization, and density of states in magnetic multilayer structures, with resolutions in the vertical coordinate, z, of a few Å [8, 9]. Our study adapts the swedge method to the PEEM, thus demonstrating the potential for measuring these same quantities with resolution in x,y, and z in future work.

Our experiments were carried out at beamline UE49-PGM-a of the BESSY facility, using an Elmitec PEEM[10] with energy filtering such that images can be based on a single

photoelectron peak. The sample was grown on a Si/$MoSi_2$ multilayer mirror consisting of 40 [Si-2.0nm/Mo-2.0nm] bilayers, and it consisted of a Ag wedge varying from about 3nm to zero in thickness over about 30 microns, on top of which were grown successively 3.3nm of Co, and 0.5nm of Au (cf. Fig. 1(a)). On top of this was a thin layer of "adventitious C" due to surface contamination. In Fig. 2(a) we show typical spectra from this sample. As expected, moving the spot from off to on the wedge turns on the various peaks from Ag. We here concentrate on images based on Ag 3*d* and C 1*s* emission, which represent the bottom and top emitter layers in the sample, and which will have a maximum phase shift relative to one another as excited by the SW.

The x-ray beam was focused to a spot with one dimension comparable to the lateral extent of the Ag wedge (cf.3 Fig 1(a)). The photon energy was adjusted to be at the 1st-order Bragg angle for the mirror, thus creating a strong standing wave (SW) in and above the mirror. The microscope geometry fixed the incidence angle at 15.7°. Using the relation $\lambda_x = 2d_{ML}\sin\theta_{Bragg}$, where λ_x = the x-ray wavelength, θ_{Bragg} = the Bragg angle and d_{ML} = 40.0Å = the mirror layer period, we obtain a photon energy of about 590eV for maximum reflectivity and maximum SW modulation. The Bragg angle was initially located by scanning photon energy and monitoring a given peak intensity (e.g. C 1*s*). At the Bragg angle, the SW period is equal to the period of the mirror [9]. The phase of the SW is also fixed with respect to the mirror surface [9]. With respect to the other layers in the sample that lie above the wedge, a given point on the SW has a vertical position z_0 which varies linearly along the wedge. Thus, we should see oscillations in the intensity of a photoelectron peak (e.g. Ag 3*d*) originating from a given depth below the surface moving along the wedge. The Ag 3*d* photoelectrons will mainly originate from the top surface of the wedge due to the finite photoelectron escape length and should exhibit such oscillations (cf. Fig. 1(b)). In Fig. 2(b), these oscillations are

experimentally observed by imaging the wedge via the Ag 3*d* and C 1*s* intensities. The images were obtained at a photon energy of 590eV, at the Bragg condition. A clear modulation of the intensities of about 20% can be seen. About one period of modulation is observed in for both core levels, as expected since the wedge height is 3.0 nm or about 75% of the SW period. There is also a clear phase shift between the modulations of the Ag 3*d* and C 1*s* intensities that is due to their different heights above the multilayer mirror which determine the SW phase: the C 1s maximum is shifted toward the upper right corner in these images.

To scan the SW through the sample layer at a fixed incidence angle we scanned the photon energy from below to above the Bragg condition. Scanning over the Bragg angle shifts the phase of the SW continuously by about one wavelength [11]. Figs. 3(a, b) summarize results from a set of images in which the photon energy was scanned in 2eV steps from 572eV to 610eV across the Bragg energy of 590eV. Ag 3*d* and C 1*s* photoemission intensities were integrated along the direction perpendicular to the wedge slope. The resulting photoelectron intensities (not shown) are found to vary as a function of position along the wedge slope and photon energy. However, to better visualize the intensity variations, we subtracted two intensity profiles across the wedge for adjacent photon energies, resulting in a derivative-like signal. In this form, the contrast of the SW intensity modulation is strongly enhanced against other sources of changes in intensity, such as photon energy-dependent cross section or electron optical effects. Such experimental intensity variations for (a) Ag 3*d* and (b) C 1*s* core levels are shown in the upper panels of Fig. 3. With increasing photon energy, the movement of the Ag 3*d* and C 1*s* intensity maxima along the wedge can nicely be observed. This movement is expected to stop at the end of the Ag wedge. This is in fact visible as a kink and a flat portion in the lower left part of the intensity modulation. The phase shifts between Ag

3*d* and C 1*s* can also clearly be seen. A video showing the actual image changes as photon energy is scanned is also available [12]. Figs. 3(c) and 3(d) show the results of x-ray optical calculations of the type used previously in swedge studies [8, 9, 13]. In these calculations, we assumed an Ag wedge height varying from 2.7nm to 0.3nm within our field of view. There is in general very good agreement between experiment and theory, including the behavior in the lower part of both images and at the top end of the wedge. Slight deviations from an ideal steep wedge profile and possibly a non-uniform C overlayer coverage due to radiation induced desorption could explain some discrepancies between experiment and theory observed for example in the upper right of Figs. 3(b) and 3(d). Overall, the calculations further confirm that we are observing depth-resolved photoemission in a single image. As concluding background to this study, we note that, in a prior investigation, standing wave excitation has been used for producing image contrast in a PEEM [14], but this study involved a much lower energy photon source at 92eV or 13.2nm wavelength and near-normal incidence, and did not include a wedge-profile layer. In this work, it was thus not possible to resolve different elements through corelevel excitation. Also, the depth resolution would be about 3 times worse (13.5/4.0) than in our study, and the lack of a wedge prevented seeing different depths in a single image.

In summary, we have shown that the standing wave/wedge (swedge) technique can be used to add quantitative depth sensitivity to element-specific soft x-ray PEEM images. Provided that a suitable sample can be grown on a multilayer mirror, this approach should yield vertical resolutions in PEEM images of the order of 1/10 of the SW period [8, 9]. Beyond the technique used here, it should be possible to make use of the swedge method in an imaging soft x-ray microscope based on Fresnel zone-plate lenses, provided that the image is created with x-ray reflection at the Bragg angle from a similar sample [15]. These methodologies

should greatly enhance the capabilities of both PEEM and x-ray microscopy as characterization tools for nanoscale structures.

Acknowledgements

C.S.F. and P.F. acknowledge support by the U.S. Department of Energy under Contract No. DE-AC02-05CH11231. C.S.F. also acknowledges support from the Alexander von Humboldt Foundation and the Helmholtz Association. The beamtime at BESSY was supported by the BMBF (FK05 ES3XBA/5) and the DFG (SFB 491). A.Kaiser thanks the DFG for the financial support within the SFB 491. We are also grateful to E. Bauer, R. Belkhou, M. Kiskinova, I. Krug, A. Locatelli, T.O. Mentes, M.A. Nino, and A. Pavlovska, for discussion and assistance during preliminary measurements at Elettra, Trieste.

References

[1] E. Bauer, Journal of Electron Spectroscopy and Related Phenomena **975**, 114 (2001).

[2] C. M. Schneider and G. Schoenhense, Reports on Progress in Physics **65**, 1785 (2002).

[3] F. Nolting, A. Scholl, J. Stöhr, J. Fompeyrine, H. Siegwart, J.-P. Locquet, S. Anders, J. Lüning, E. E. Fullerton, M. F. Toney, M. R. Scheinfein, and H. A. Padmore, Nature **405**, 767 (2000).

[4] H. Ohldag, A. Scholl, F. Nolting, S. Anders, F. U. Hillebrecht, and J. Stöhr, Phys. Rev. Lett. **86**, 2878 (2001).

[5] S.-B-Choe, Y. Acremann, A. Scholl, A. Bauer, A. Doran, J. Stöhr, and H. Padmore, Science **304**, 420 (2004).

[6] B. Mesler, P. Fischer, W. Chao, E. Anderson, and D. Kim, J. Vac. Sci. Tech. B **25**, 2598 (2007).

[7] R. Fink, M. R. Weiss, E. Umbach, D. Preikszas, H. Rose, R. Spehr, P. Hartel, W. Engel, R. Degenhardt, R. Wichtendahl, H. Kuhlenbeck, W. Erlebach, K. Ihmann, R. Schlögl, H. -J. Freund, A. M. Bradshaw, G. Lilienkamp, Th. Schmidt, E. Bauer, and G. Benner., Journal of Electron Spectroscopy and Related Phenomena **84**, 231 (1997).

[8] S. Yang, B. Mun, , and C. Fadley, Synch. Rad. News **17**, 24 (2004).

[9] S.-H. Yang, B. Sell, and C. S. Fadley, J. Appl. Phys. **103**, 07C519 (2008).

[10] F. Kronast, R. Ovsyannikov, H.A. Dürr, and W. Eberhardt, to be published.

[11] J. Woicik, Inst. and Meth. in Phys. Res. A **547**, 227 (2005).

[12] A video illustrating the movement of both of these images, and the phase shift between them, as photon energy is scanned in 2 eV steps from 572 eV to 606 eV is available at http://www.physics.ucdavis.edu/fadleygroup.

[13] S. Y. S. written computer program for simulating photoemission intensities with standing waves created in reection from a multilayer mirror., to be published.

[14] J. Lin, U. Neuhaeusler, J. Slieh, A. Brechling, U. Kleineberg, U. Heinzmann, A. Oelsner, D. Valdaitsev, G. Schoenhense, N. Weber, M. Escher, and M. Merkel, J. Vac. Sci. Tech. B **24**, 2631 (2006).

[15] P. Fischer and C. Fadley, unpublished results.

Figure captions:

FIG. 1: (color online) Two views of our implementation of the standing wave/wedge (swedge) method in a photoelectron microscope, for the specific case of a Ag wedge below Co and Au layers, and with a C contaminant layer on top. The x-ray spot is elongated in one direction due to the low incidence angle of 15.7°.

FIG. 2: (color online) : (a) Typical broad-scan photoelectron spectra from the sample in Fig. 1 obtained in the PEEM with the x-ray spot on and off the Ag wedge. The Ag 3*d* and C 1*s* intensities were used in the images which follow. (b) The difference of two PEEM images taken well above (602eV) and on the Bragg reflection condition (590eV) using (a) the Ag 3*d* and (b) the C 1*s* intensities to produce the image. The difference images show a 20% modulation of photoemission intensity introduced by the SW. Both difference images are normalized to the intensity distribution at 602eV . Note the phase shift between the two images due to the different vertical positions of C and Ag with respect to the multilayer mirror which generates the standing wave. See also [12].

FIG. 3: (color online): Summary of Ag 3*d* and C 1*s* intensities as integrated along a direction perpendicular to the long axis of the x-ray spot, for all 18 energies between 572 and 610eV . The upper parts (a) and (b) display the derivative of experimental Ag 3*d* and C 1*s* intensity modulations introduced by the SW while the photon energy is scanned across the Bragg condition. The lower parts (c) and (d) show x-ray optical simulations of the experimental results. The simulations assumed the geometry shown in Fig. 1, including a 2.7nm high Ag

wedge (independently determined by AFM profilometry) and finally the same derivative procedure as in (a) and (b).

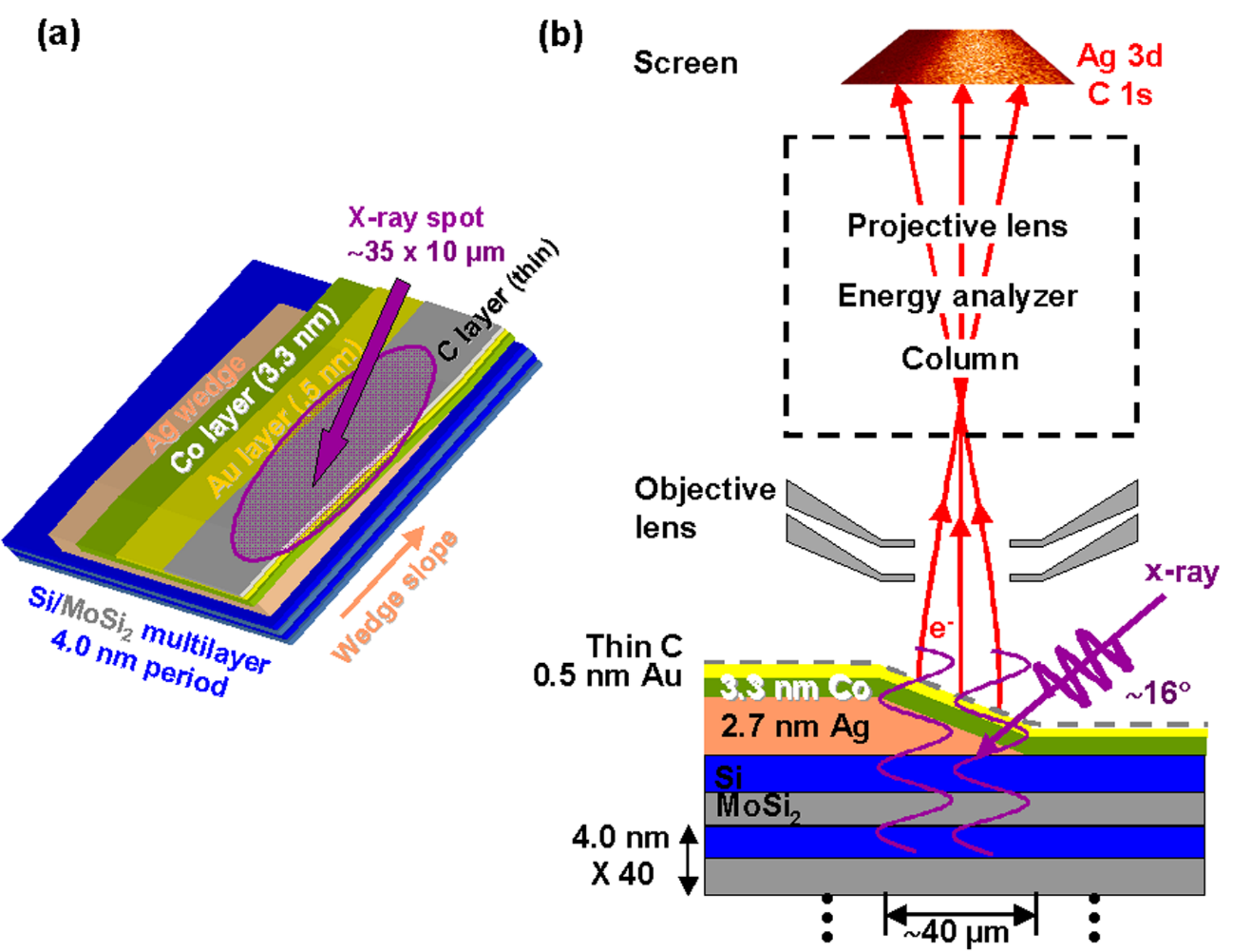
(a)
X-ray spot
~35 x 10 μm
C layer (thin)
Ag wedge
Co layer (3.3 nm)
Au layer (.5 nm)
Wedge slope
Si/MoSi2 multilayer
4.0 nm period
(b)
Screen
Ag 3d
C 1s
Projective lens
Energy analyzer
Column
Objective lens
x-ray
e-
Thin C
0.5 nm Au
3.3 nm Co
2.7 nm Ag
Si
MoSi2
~16°
4.0 nm
X 40
~40 μm

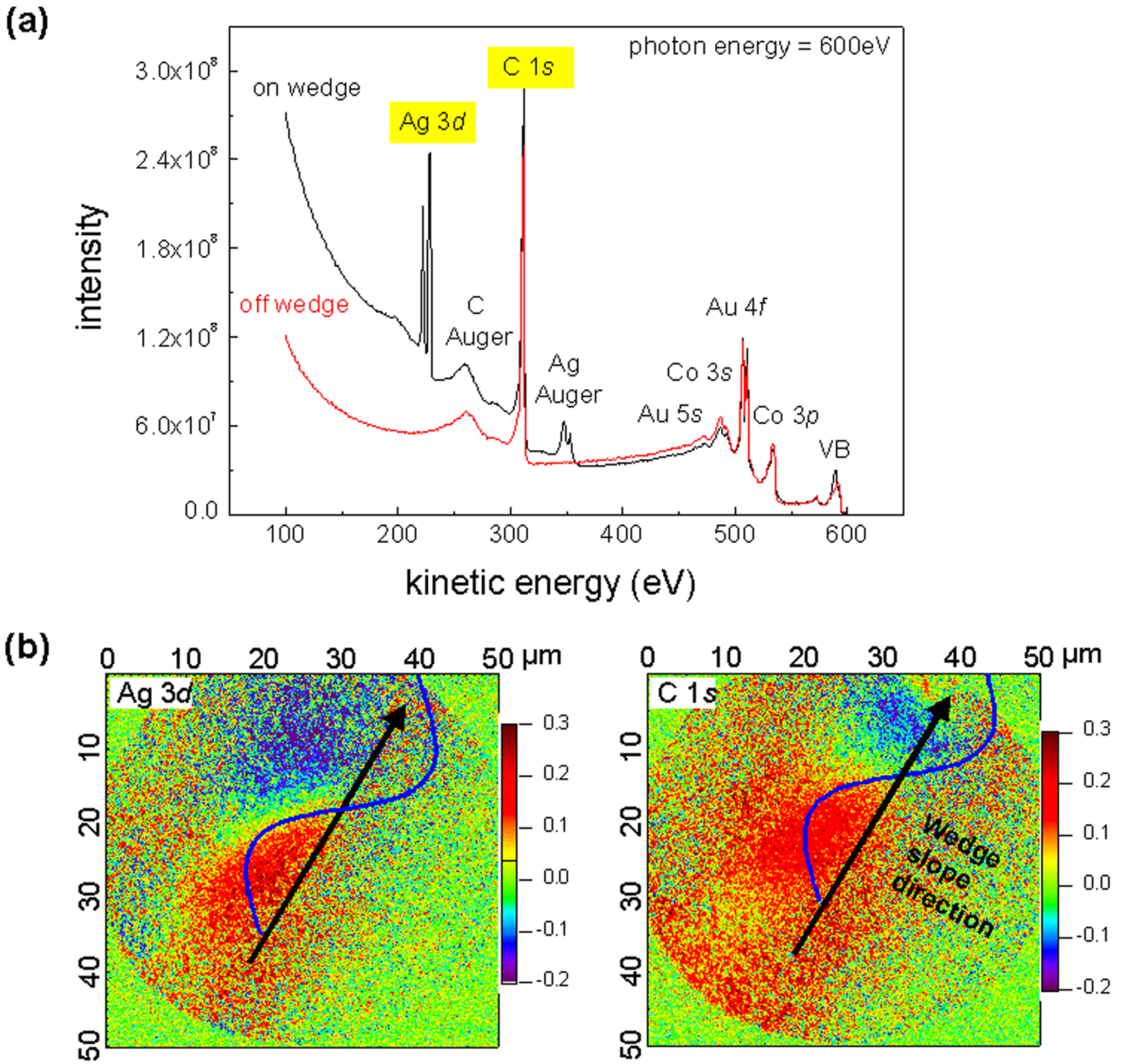
(a)
photon energy = 600eV
on wedge
off wedge
C 1s
Ag 3d
C Auger
Ag Auger
Au 4f
Co 3s
Au 5s
Co 3p
VB
intensity
kinetic energy (eV)
3.0x10^8
2.4x10^8
1.8x10^8
1.2x10^8
6.0x10^7
0.0
100
200
300
400
500
600
(b)
Ag 3d
C 1s
0
10
20
30
40
50 μm
0.3
0.2
0.1
0.0
-0.1
-0.2
Wedge slope direction

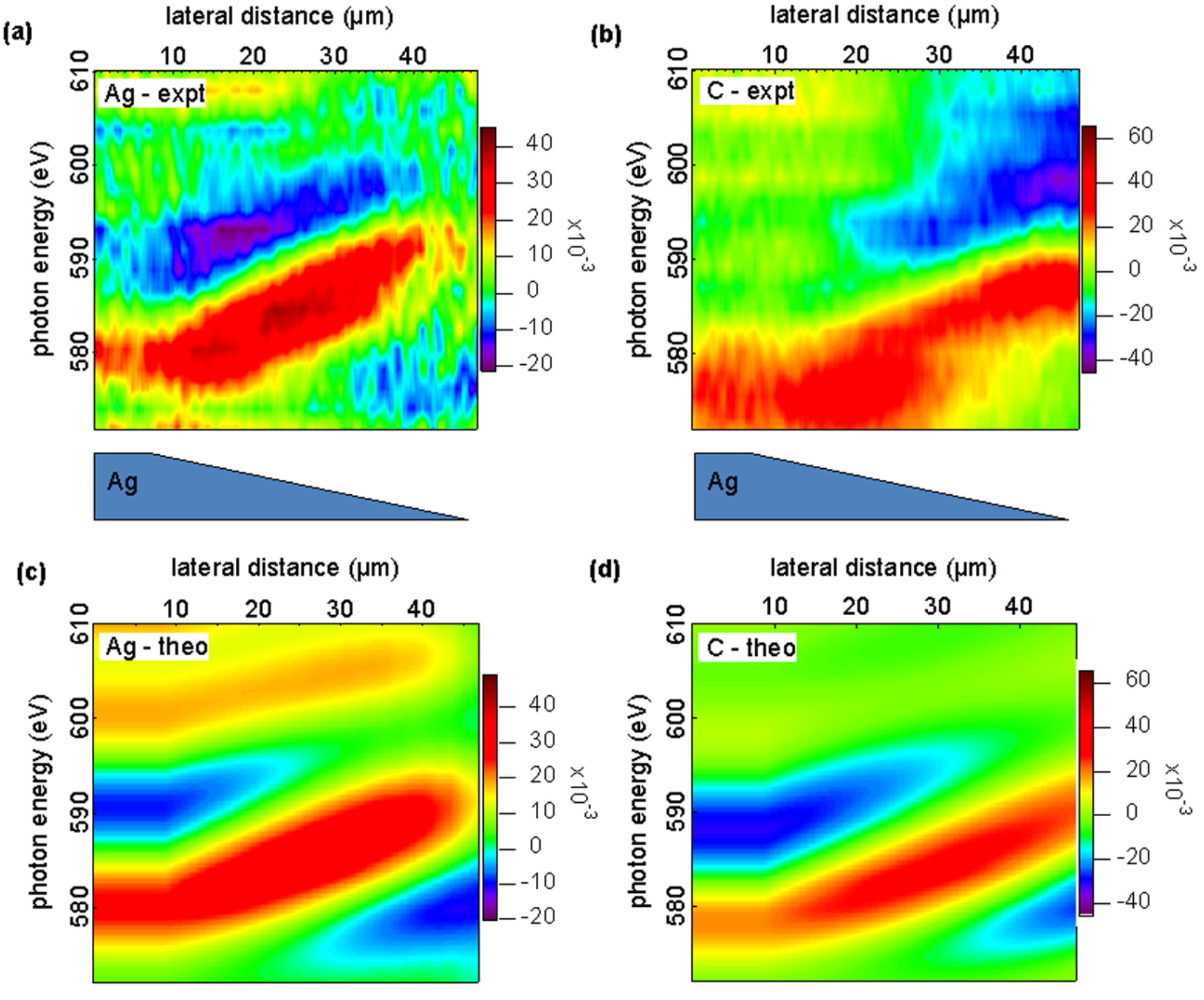
(a)
lateral distance (μm)
10
20
30
40
610
600
590
580
photon energy (eV)
Ag - expt
40
30
20
10
0
-10
-20
x10-3
Ag
(b)
lateral distance (μm)
C - expt
60
40
20
0
-20
-40
Ag
(c)
Ag - theo
(d)
C - theo